Carbon nanotube biconvex microcavities

Haider Butt, Ali K. Yetisen, Rajib Ahmed, Seok Hyun Yun, and Qing Dai

View Online   Export Citation   CrossMark

AIP
Publishing

106, 121108

Carbon nanotube biconvex microcavities

Haider Butt,[1,a)] Ali K. Yetisen,[2] Rajib Ahmed,[1] Seok Hyun Yun,[2] and Qing Dai[3]
[1]*Nanotechnology Laboratory, School of Mechanical Engineering, University of Birmingham, Birmingham B15 2TT, United Kingdom*
[2]*Harvard Medical School and Wellman Center for Photomedicine, Massachusetts General Hospital, 50 Blossom Street, Boston, Massachusetts 02114, USA*
[3]*National Center for Nanoscience and Technology, Beijing 100190, China*

Developing highly efficient microcavities with predictive narrow-band resonance frequencies using the least amount of material will allow the applications in nonlinear photonic devices. We have developed a microcavity array that comprised multi-walled carbon nanotubes (MWCNT) organized in a biconvex pattern. The finite element model allowed designing microcavity arrays with predictive transmission properties and assessing the effects of the microarray geometry. The microcavity array demonstrated negative index and produced high Q factors. 2–3 μm tall MWCNTs were patterned as biconvex microcavities, which were separated by 10 μm in an array. The microcavity was iridescent and had optical control over the diffracted elliptical patterns with a far-field pattern, whose properties were predicted by the model. It is anticipated that the MWCNT biconvex microcavities will have implications for the development of highly efficient lenses, metamaterial antennas, and photonic circuits. © 2015 AIP Publishing LLC. [http://dx.doi.org/10.1063/1.4916236]

Multi-walled carbon nanotubes (MWCNTs) were first reported by Iijima in 1991[1] and since then they have been the focus of significant research to develop a myriad of applications in photonics, energy storage, and biotechnology. MWCNTs are structurally analogous to the concentric arrays of cylindrical tubes made out of single graphite sheets. They are mostly metallic and are able to carry high current densities, which allow their utilization in electronics including field emission displays, rectifier electrodes, solar cells, and optical antenna arrays.[2] The unique optical properties of MWCNTs have also been explored in numerous applications such as plasmonic nanotweezers,[3] photonic crystals, metamaterials,[4] and diffraction gratings.[5] Individual MWCNTs display a frequency dependent dielectric function, which is anisotropic in nature and closely matches with that of bulk graphite. However, the dense periodic arrays of MWCNTs may display an artificial dielectric function, with a lower effective plasma frequency in a few hundreds of terahertz, acting as metamaterials.[6]

Microcavities are an emerging area of research due to their ability to confine light to low volumes by resonant recirculation and filter out specific wavelengths for applications in optoelectronics, quantum computing, and lasers.[7] Microcavities have been fabricated by forming photonic crystals that incorporated point defects within the periodic lattice structures.[8] Within the band gaps frequency ranges, the light coupled into the cavity cannot enter the rest of the lattice, and hence high Q factors can be achieved. Other approaches included circular disk microcavities, which acted as ring resonators and could couple/filter light from waveguides.[9] Furthermore, CNT photonic crystal lenses that exhibited negative index have been demonstrated.[10] In photonic crystals, when the size and periodicity of the scattering elements are on the order of the wavelength of incident light,

Bragg diffraction occurs due to light interference in periodic regions.[11] The diffraction in photonic crystals excites waves, where the phase and group velocities are reversed in the same manner as in negative index metamaterials. Thus, under the right conditions, negative refraction can be observed in photonic crystals.[12] However, achieving the attributes of a microcavity array with predictive narrow-band filtering properties still remains a significant challenge. Harnessing the optical advantages of negative index properties and utilization of MWCNT arrays to construct microcavities can lead to applications in waveguides, optoelectronics, photovoltaics, and photodetectors.

Here, we present an efficient strategy for the design and fabrication of photonic MWCNT microcavities with high Q factors. By combining the advantages of finite element modeling and an optimized nanopatterning technique, we produced MWCNT regions that were organized in a biconvex microcavity array, which allowed filtering out specific incident wavelengths anywhere from the visible spectrum to near infrared. The simulated model allowed assessing the effect of microcavity configuration on the transmitted light, hence provided an efficiency approach for predicting the optical properties. After the optimization of optical properties, biconvex MWCNT arrays were fabricated at nanoscale spacings to construct an efficient microcavity. The microcavity provided optical control over the diffracted elliptical patterns with an envelope of far-field pattern, whose properties were predicted by the simulations.

Computational modeling allowed the evaluation of the optical characteristics of the MWCNT array due to changes in nanotube organization, periodicity, and size.

The negative dielectric property displayed by the arrays of MWCNTs can be utilized to establish optical microcavities and resonators.[6,10] High density arrays of metal wires with 1D periodicity have been shown to display plasmonic properties.[13] When the ratio of diameter to distance between

---

a)Email: h.butt@bham.ac.uk. Tel.: +441214158623.

the metal wires was increased, a transition from a metallic photonic to a plasmonic crystal was obtained. Transmission of the incoming electromagnetic waves was strongly influenced by surface plasmons and mutual coupling between the wires, leading to a plasmonic behavior with an effective plasma frequency. Such 1D arrays of metal wires displayed artificial negative dielectric constants toward incident electromagnetic waves. The same effect can be produced by carbon nanotubes organized in arrays. Single rows of closely spaced MWCNTs act as reflectors toward the incident light and can be utilized to construct light-trapping optical microcavities.

The structures were modeled by using the geometries analogous to the negative-index biconvex lenses demonstrated in our previous paper.[10] MWCNTs organized as a biconvex lens with a centered vertical row were designed to model the optical microcavities. Figure 1 shows the finite element method (FEM) analysis of optical transmission through the MWCNT biconvex cavity. For simplicity, a 2D geometry of MWCNTs was considered and the electromagnetic field was assumed to be invariant along the axis of the nanotubes (z axis). This assumption holds as long as the tube height is several times larger than the operating wavelength. The dielectric constant of the MWCNT was obtained from the Drude-Lorentz model[6] and was incorporated into the model as a frequency dependent function. The calculations were performed for the light polarized parallel to the MWCNTs (transverse electric).

The frequency modes having wavelengths comparable to the MWCNT cavity structure showed strong resonates. A high resonance was observed at 1970 nm in the optical cavity with a $2 \mu m$ base (Fig. 1(b)). The cavity displayed a Q factor of the order 133, which may be further increased by optimizing the geometry. This is on interest here and it shows that by using this model, the microcavities can be designed in different configurations to predict the optical characteristics and transmission spectra. Additionally, unlike the photonic crystals cavities, which require nanopatterning over large area, the demonstrated microcavities are practical, require less material, and reduce nanofabrication steps.

To obtain the resonance in the visible regime, a thinner optical cavity with a 800 nm base was modeled (Fig. 2(a)).

The resonance wavelengths of the cavity were found at 385, 560, and 670 nm due to photonic band-gap effects (Figs. 2(b) and 2(c)). The cavity behaved like a Fabry–Pérot cavity with the resonant modes depending on its geometry and dimensions. As shown in Fig. 2(b), a relation was observed between the resonant modes and the vertical dimension of the cavity. The 385 nm wave resonated within a cavity region of height $5a$ ($a = 400$ nm) as $385 \times 5.2 \approx 5a$, whereas the 560 nm wave resonated throughout the height of the cavity as $560 \times 5 = 7a$ and 670 nm wave resonated at a distance of $5a$ ($\sim 3 \times 670$). The strength of the resonant modes decreased as the wavelength increased.

Further studies were performed to understand the dependence of the resonance wavelengths on the geometrical features such as the CNT radius r and lattice constant a. As shown in Fig. 3(a), increase in the CNT radius blue shifted the peaks. The resonant peak which was originally at 385 nm for $r = 50$ nm shifted to 375, 365, and 320 nm for r = 55, 60, and 65 nm, respectively. This can be attributed to the increase in fill factor due to increasing CNT radius and the lack of empty space within the cavity. Also for larger CNT radii, lower resonance intensities were observed, which could be due to the intensity distribution to the extra side lobes (at smaller resonances wavelength). Hence, the geometries with smaller CNT radii are desirable to achieve intense and narrow band resonance peaks, but the fabrication complexity and quality tradeoffs need to be considered.

The micro cavity was designed with a vertical lattice spacing a of 400 nm and the horizontal spacings were set as 75%, 50%, and 100% of a for the 2nd, 3rd, and 4th rows, respectively. The lattice constant was varied to expand and contract the microcavity and its resonance was studied (Fig. 3(b)). The general trend observed was the red shift of resonant peaks with expanding lattice spacing. For the lattice spacing below 440 nm, around three resonant peaks were observed. For $a = 440$ nm, a greater number of resonant modes were observed owing to have more space within the cavity. However, the resonant modes for smaller wavelengths generally presented higher intensities.

In addition, the simulation of far-field diffraction allowed the pattern analysis of the scattered light from a MWCNT microcavity array (Fig. 4(a)). Figure 5(b) illustrates the diffraction pattern for a normally incident beam
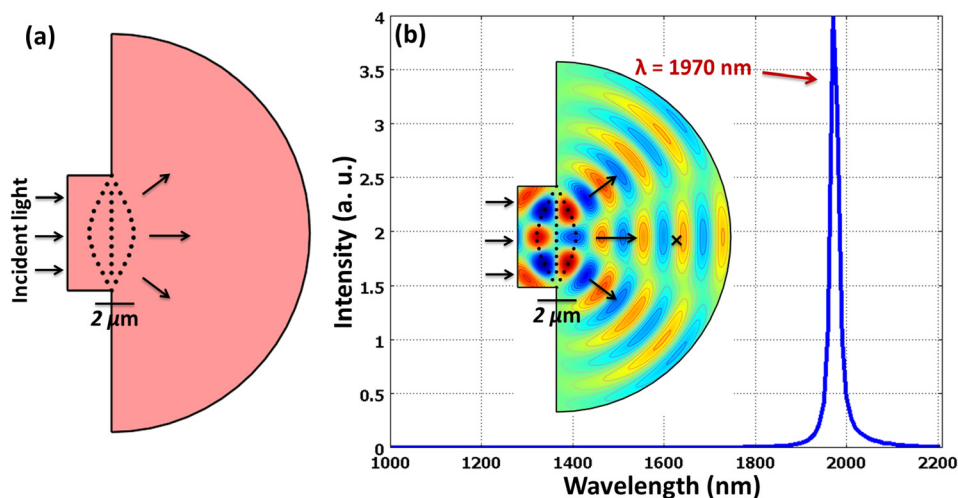

FIG. 1. Computational model of MWCNT optical microcavity with vertical lattice spacing $a = 400$ nm and $r = 50$ nm. (a) $2 \mu m$ wide microcavity based on curved rows of nanotubes which acted as reflectors. (b) Wave propagation and transmission spectrum collected from the crossed region showed high resonance at $\sim 2 \mu m$.
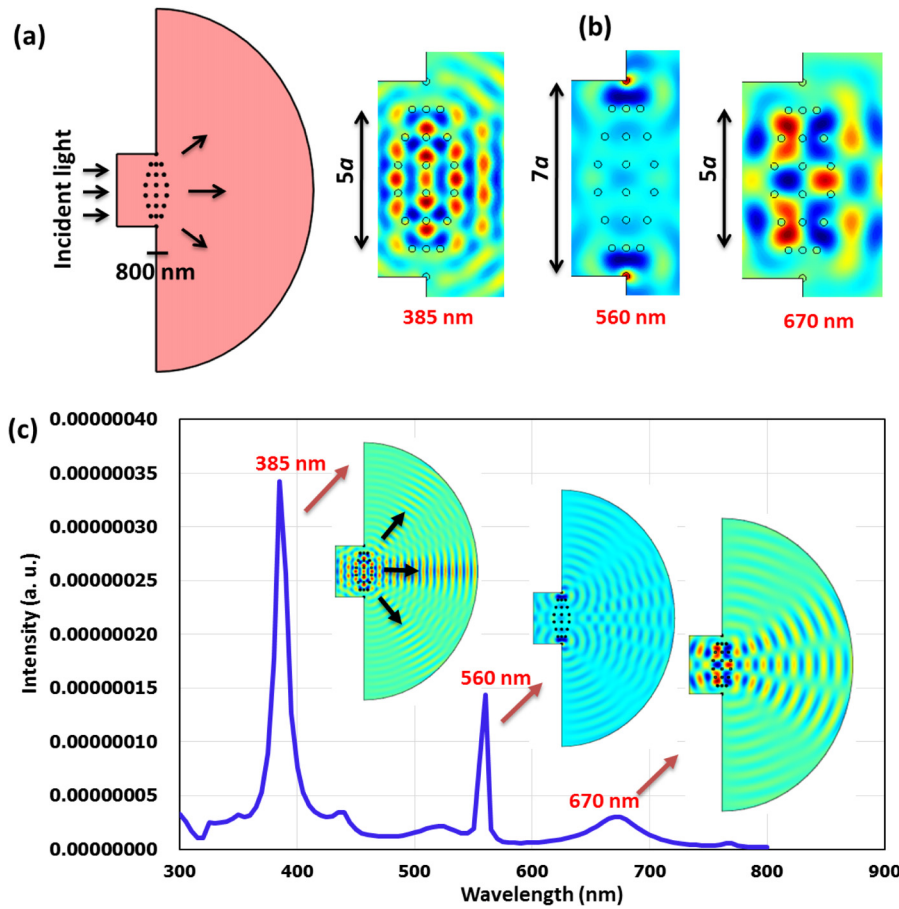
FIG. 2. (a) The geometry of a thinner 800 nm wide microcavity with vertical lattice spacing $a = 400$ nm and $r = 50$ nm. (b) Magnified view of the microcavity at its resonant modes at 385, 560, and 670 nm. (c) Transmission spectrum for the thinner microcavity with inset showing the radiation patterns of the resonant modes.

reflected from the microcavity array. In the model, the diffractive elements (MWCNTs) were considered as a 2D Dirac delta array, which implied that the nanotube did not have any intrinsic 3D shape in the simulation. According to the Fourier theory, the shapes of the unit diffractive element (the MWCNTs and microcavities) have an effect on the overall envelope of the far-field pattern. Due to the normal incidence of light, this effect was minimal in the simulation. The

computed diffraction pattern in Fig. 4(b) consisted of several continuous features, most prominent of which were an array of ellipses resembling the microcavities. These orthogonally aligned (horizontal) ellipses represented the Fourier transform of the individual microcavities, which were vertical configurations. Figure 4(b) also shows a circular envelop encompassing the diffraction patterns, which is due to the biconvex shape of the MWCNTs.
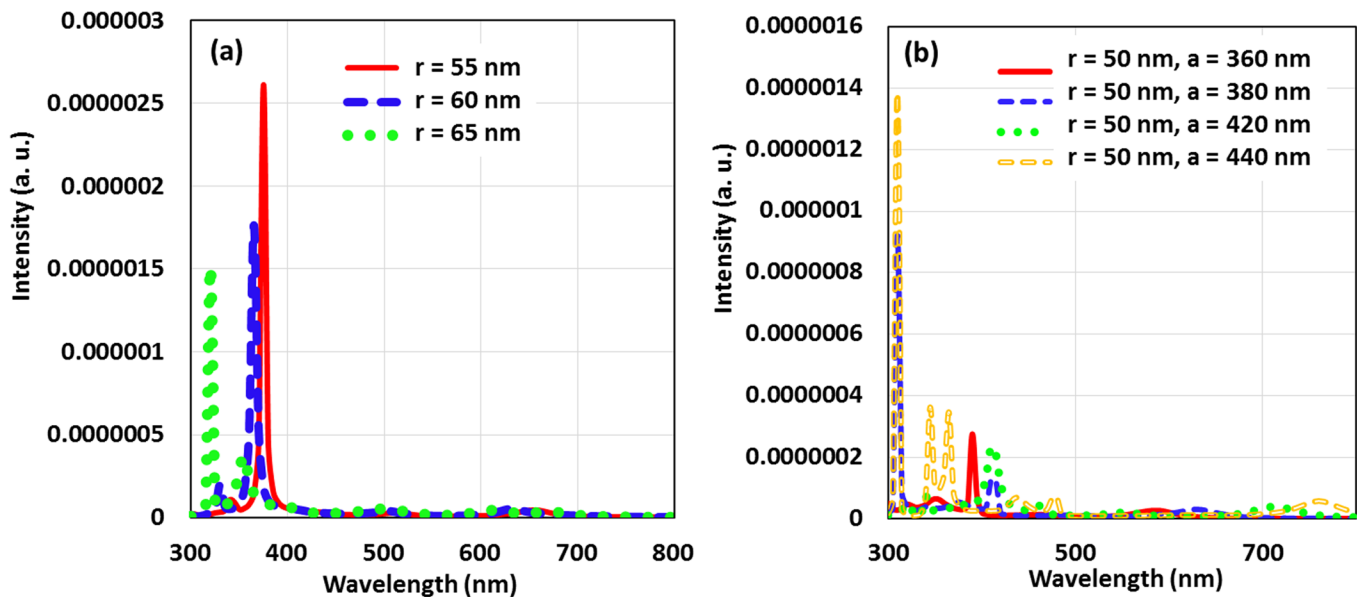

FIG. 3. (a) The effect on cavity resonance with varying CNT radius. (b) Resonance for a varying lattice constant a with CNT radius of 50 nm.
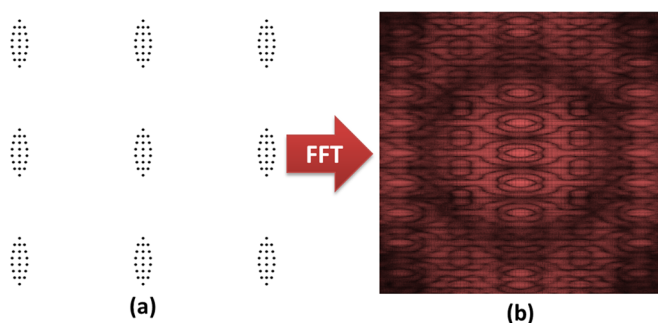
FIG. 4. Simulated far-field diffraction of the MWCNT microcavity. (a) The designed model of 2D array. (b) 2D fast Fourier transform (FFT) of the microcavity array producing a diffraction pattern consisting of orthogonally arranged ellipses and a circular features.

The biconvex cavity arrays were patterned on a Si substrate using plasma-enhanced chemical vapor deposition (PECVD). Electron-beam lithography was used to pattern a 5 nm thick Ni catalyst layer into an array, in which the diameter of each dot was 100 nm. This allowed the growth of a single MWCNT with 50 nm radius on each dot. An optimized PECVD growth recipe (reported in Ref. 6) lasted for about 10–15 min at 725 °C and produced ~2–3 μm tall

MWCNTs. Figure 5 shows the SEM images of the microcavity array and a MWCNT island. The fabrication required the MWCNTs growth at a spacing ranging from 100 to 400 nm.

Strong diffraction effects were observed from the fabricated microcavity arrays, which were iridescent (Fig. 6(a)). The diffraction patterns from the microcavity array were characterized by illuminating the sample positioned onto a goniometer by a He-Ne laser (632.8 nm) from an incidence angle of ~40° (Fig. 6(b)). The background screen was placed at ~30 cm away from the sample, and the intensity patterns of light on the screen were captured with a digital single-lens reflex (DSLR) camera. As the spacing between the MWCNTs was of the order of the incident wavelength, the first order diffracted light was expected at wide angles of ~60° from the zero order (reflected beam). Figures 6(c) and 6(d) show the photographs of the diffraction patterns, which are in agreement with the simulated far field patterns. The pattern consisted of an array of spots representing an individual optical cavity, and the zero order was observed in the center of the screen. The array of spots was curved as the 3D diffraction pattern was imaged on a plane surface. The inset in Fig. 6(c) shows the intensity distribution across the central arc of the diffraction pattern. The diffraction intensity is symmetrically distributed at the spots around the zero order.
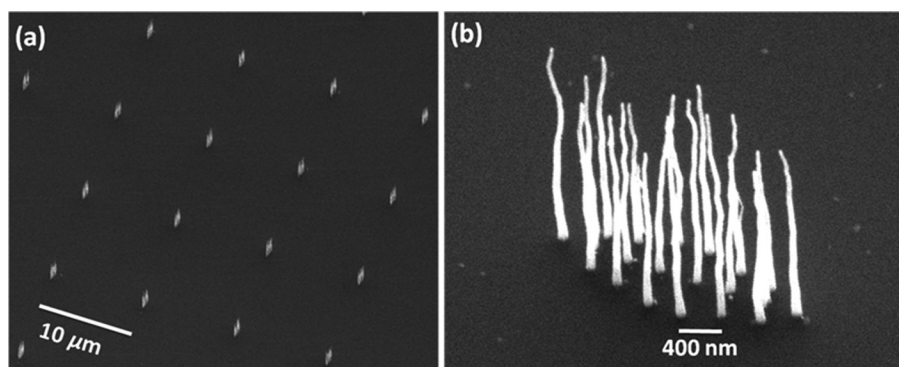

FIG. 5. SEM images of MWCNT arrays. (a) An array of MWCNT optical microcavities grown at 10 μm spacing and (b) a biconvex microcavity.
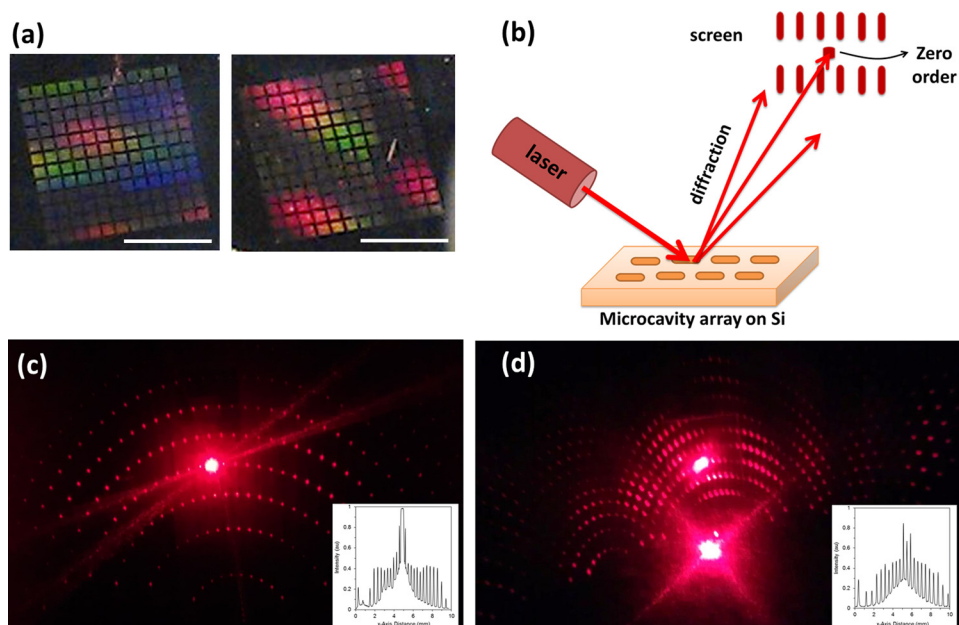

FIG. 6. Optical characterization of the MWCNTs microcavities. (a) The fabricated samples showing iridescence. The scale bars represent 0.5 mm. (b) The schematic of the experimental setup for characterizing the optical properties. (c) Diffraction pattern produced by the microcavity array. The inset shows the intensity distribution across the central arc. (d) The diffracted pattern from a different view.

Figure 6(d) shows a larger view of the diffraction pattern, and an envelope encompassing the diffraction was observed, which was predicted by the microcavity model.

MWCNT microcavities were also spectrally characterized by using a spectrometer positioned on a goniometer, which allowed reflection measurements at different angles. However, due to the small size of the microcavities, reflection measurements were not substantial. The arrays of microcavities were patterned at a spacing of 10 μm, which caused >90% free area over the Si substrate. A considerable intensity of the incident light was reflected from the unpatterned regions of Si substrate as the first order light. An advanced experimental setup will be required for the accurate experimental characterization of these microcavities. As a future work, these microcavities should be fabricated along with the in-plane Si optical waveguides on both sides of the patterned regions. Light may be coupled in/out of these in-plane Si waveguides. In-plane spectral measurements will accurately reveal the resonant frequency modes of the MWCNT microcavities.

We demonstrated a MWCNT biconvex microcavity array, which displayed promising Q factors. The microcavity array acted like an optical antenna that supported several resonating modes anywhere from the visible spectrum to near infrared. The resonant frequencies were controlled by finely changing the MWCNT microcavity geometry. We have shown that by using our computational model, the resonant modes and Q factors can be engineered and optimized for the desired optical patterns and transmission spectra. The fabricated biconvex microcavities showed strong interaction with the incident light and its diffraction effects were analyzed. The demonstrated microcavities are unique as they display strong optical resonances while requiring minimum material for their fabrication as compared to the existing fabrication approaches. We anticipate that the MWCNT biconvex microarrays will lead to applications in tunable lasers, electro-optic modulation, and nanophotonic circuits.

[1] S. Iijima, Nature **354**(6348), 56 (1991).

[2] K. Jensen, J. Weldon, H. Garcia, and A. Zettl, Nano Lett. **7**(11), 3508 (2007).

[3] D. Dell, X. Serey, and D. Erickson, Appl. Phys. Lett. **104**(4), 043112 (2014).

[4] H. Butt, Q. Dai, P. Farah, T. Butler, T. D. Wilkinson, J. J. Baumberg, and G. A. J. Amaratunga, Appl. Phys. Lett. **97**(16), 163102 (2010).

[5] K. Won, A. Palani, H. Butt, P. J. W. Hands, R. Rajesekharan, Q. Dai, A. Ahmed Khan, G. A. J. Amaratunga, H. J. Coles, and T. D. Wilkinson, Adv. Opt. Mater. **1**(5), 368 (2013).

[6] H. Butt, Q. Dai, R. Rajesekharan, T. D. Wilkinson, and G. A. J. Amaratunga, ACS Nano **5**(11), 9138 (2011).

[7] G. Cui, J. M. Hannigan, R. Loeckenhoff, F. M. Matinaga, M. G. Raymer, S. Bhongale, M. Holland, S. Mosor, S. Chatterjee, H. M. Gibbs *et al.*, Opt. Express **14**(6), 2289 (2006); J. Ma, J. Ju, L. Jin, W. Jin, and D. Wang, *ibid.* **19**(13), 12418 (2011).

[8] W. C. L. Hopman, K. O. van der Werf, A. J. F. Hollink, W. Bogaerts, V. Subramaniam, and R. M. de Ridder, Opt. Express **14**(19), 8745 (2006).

[9] K. J. Vahala, Nature **424**(6950), 839 (2003); X.-F. Jiang, Y.-F. Xiao, C.-L. Zou, L. He, C.-H. Dong, B.-B. Li, Y. Li, F.-W. Sun, L. Yang, and Q. Gong, Adv. Mater. **24**(35), OP260 (2012).

[10] H. Butt, Q. Dai, T. D. Wilkinson, and G. A. J. Amaratunga, Photonics Nanostruct.: Fundam. Appl. **10**(4), 499 (2012).

[11] X.-T. Kong, H. Butt, A. K. Yetisen, C. Kangwanwatana, Y. Montelongo, S. Deng, F. da Cruz Vasconcellos, M. M. Qasim, T. D. Wilkinson, and Q. Dai, Appl. Phys. Lett. **105**(5), 053108 (2014); F. da Cruz Vasconcellos, A. K. Yetisen, Y. Montelongo, H. Butt, A. Grigore, C. A. B. Davidson, J. Blyth, M. J. Monteiro, T. D. Wilkinson, and C. R. Lowe, ACS Photonics **1**(6), 489 (2014); A. K. Yetisen, H. Butt, F. da Cruz Vasconcellos, Y. Montelongo, C. A. B. Davidson, J. Blyth, L. Chan, J. Bryan Carmody, S. Vignolini, U. Steiner *et al.*, Adv. Opt. Mater. **2**(3), 250 (2014); C. P. Tsangarides, A. K. Yetisen, F. da Cruz Vasconcellos, Y. Montelongo, M. M. Qasim, T. D. Wilkinson, C. R. Lowe, and H. Butt, RSC Adv. **4**(21), 10454 (2014); A. K. Yetisen, M. M. Qasim, S. Nosheen, T. D. Wilkinson, and C. R. Lowe, J. Mater. Chem. C **2**(18), 3569 (2014).

[12] D. R. Smith, J. B. Pendry, and M. C. K. Wiltshire, Science **305**(5685), 788 (2004).

[13] C. R. Simovski, P. A. Belov, A. V. Atrashchenko, and Y. S. Kivshar, Adv. Mater. **24**(31), 4229 (2012).